

中国激光

高速气流下激光辐照金属平板热-力响应尺度律研究

崔悦^{1,3}, 王睿星^{1,3*}, 马特^{1,3}, 袁武^{1,2,3}, 宋宏伟^{1,2,3}, 黄晨光³

¹中国科学院力学研究所流固耦合系统力学重点实验室, 北京 100190;

²中国科学院力学研究所空天飞行高温气动国家重点实验室, 北京 100190;

³中国科学院大学工程科学学院, 北京 100049

摘要 高速气流作用下激光辐照结构诱导的热-力响应相似关系, 因涉及多物理场之间的强耦合而非常复杂。笔者采用近似等效方法, 将切向气流的作用等效为金属平板结构的力载荷和热载荷边界条件, 建立了该耦合问题的无量纲控制方程, 并结合主控因素分析, 推导出了适用于高速气流与激光联合作用下的金属平板热-力响应特性的相似关系与尺度律。采用高速气流下强激光辐照金属平板的流-热-固多场耦合数值算例对该尺度律进行考核验证, 结果表明: 不同缩比率及不同马赫数条件下, 满足该相似关系的缩比模型与原模型之间的热-力响应误差均在 1% 之内。本研究为高速气流条件下激光辐照缩比模型近似等效试验的开展奠定了理论基础。

关键词 激光技术; 尺度律; 方程分析法; 金属平板; 多场耦合; 热-力响应

中图分类号 TN249 文献标志码 A

DOI: 10.3788/CJL231077

1 引言

激光技术在增材制造、去除加工、武器效应等领域应用越来越广泛^[1-7]。特别地, 激光武器具有瞬时打击、转移迅速等优点, 在拦截高速目标方面具有独特优势。开展高速气流下激光辐照试验研究, “进”可为激光高效毁伤策略提供理论依据, “退”可为飞行器的激光防护提供基础支撑, 对我国空天攻防体系发展具有重要意义。然而, 高速气流条件下激光辐照试验研究受装备条件和试验环境的限制, 往往很难针对大型工程结构开展全尺寸模型试验; 即便是满足全尺寸模型试验条件, 也会因试验成本高、周期长, 很难系统地完成研究工作, 通常需要依靠大量的缩比模型试验来完成规律性研究^[8-10]。因此, 有必要开展高速气流下激光诱导的热-力响应尺度律研究, 从而为激光辐照缩比试验提供必要的理论支撑。

静态空气环境下激光诱导的热-力响应相似理论已经取得了一定进展。陈发良等^[11]从理论上探讨了热-力耦合问题的尺度关系, 发现温度-变形耦合项的存在导致该问题无法满足几何相似律。然而, 准静态加载速率条件下的变形功引起的内能变化可以忽略, 因此一般可忽略此耦合项; 反过来, 即便是在很高的升温速率下, 由热膨胀产生的惯性力对平衡方程的影响也可以忽略^[12]。黄晨光等^[13]和马特等^[14]采用方程分析法, 从理论上推导了激光辐照下承受复杂热-力载荷的

圆柱壳结构的相似律。在试验研究方面, 王玉恒等^[15]和李成龙等^[16]通过缩比试验测试探究了同一加载条件和不同缩比率下的相似性规律。刘坤等^[17]通过开展缩比实验及修正实验, 建立了激光对航空铝合金材料的毁伤模型经验公式。然而, 上述研究大多是针对静态空气环境下的激光辐照效应相似理论开展的。高速切向气流下的激光辐照效应涉及流场(流)、温度场(热)、变形场(固)多物理场之间的强耦合效应, 导致结构热-力响应特性与静态空气条件下的^[1-3, 18-19]有显著区别, 上述相似准则不再适用。

当前对于流-热-固多场耦合条件下的相似关系的研究大多集中在高超声速飞行器分析与设计领域。由于多场耦合问题的复杂性, 往往不存在满足所有条件的完全相似准则。此时, 剔清主控参量, 忽略不关键因素的影响, 建立满足关键条件的近似等效相似准则, 是研究多场耦合问题相似理论的有效途径。一种常见的处理方式是将高速气流诱导的气动力/热效应等效为热-力载荷加载到结构表面。基于此, 刘磊等^[20]针对高超声速飞行器热气弹问题相似准则进行了推导, 把多场耦合相似问题简化为热-力耦合相似问题, 给出了热防护结构地面考核试验的相似准则, 但他们未考虑流动的相似性。Ai 等^[21]同时考虑流动与结构热传导的相似关系, 建立了气动和传热耦合条件下结构温度响应的尺度律, 但是忽略了气动力、结构变形等因素的影响。总的来说, 当前针对流-热-固多物理场耦合条件

收稿日期: 2023-08-01; 修回日期: 2023-08-25; 录用日期: 2023-09-05; 网络首发日期: 2023-09-15

基金项目: 国家自然科学基金(11902322, 12272379, 12232020)

通信作者: *wangruixing@imech.ac.cn

下的相似理论研究还比较有限,仍未形成深入、系统的认识。对于高速气流条件下激光辐照结构热-力响应问题,激光辐照带来的局部高热流特征进一步加剧了流-热-固多场耦合效应,相关条件下的相似理论和尺度律有必要开展进一步的研究。

基于此,笔者针对高速气流与激光联合作用下金属平板热-力响应特性相似理论开展研究,通过方程分析法推导得到了激光-气流-传热-结构耦合条件下的近似等效尺度律,以期为高速气流环境下的激光辐照试验和效应规律研究提供基础性支撑。

2 基本控制方程与相似准则理论分析

2.1 基本控制方程

结构内部的温度场分布规律可由热扩散方程表征,在不考虑内热源的情况下,直角坐标系下各向同性材料的瞬态热传导方程^[11-12]可以简化为

$$\frac{\partial T}{\partial t} = \frac{k}{\rho C} \nabla^2 T, \quad (1)$$

式中:T为热力学温度;t为时间;k为材料的热导率;ρ为材料密度;C为材料的比热容;∇²为拉普拉斯算子。

应力场分布规律由热弹性控制方程表征,对于各向同性材料,此处采用张量形式的三维理想热弹性静力学方程组。该基本方程组包括平衡方程、几何方程、本构方程,它们的表达式分别为

$$\sigma_{ji,j} + f_i = 0, \quad (2)$$

$$\epsilon_{ij} = \frac{1}{2}(\mathbf{u}_{i,j} + \mathbf{u}_{j,i}), \quad (3)$$

$$\sigma_{ij} = \lambda \epsilon_{kk} \delta_{ij} + 2G \epsilon_{ij} - \frac{E}{1-2\nu} \alpha (T - T_0) \delta_{ij}, \quad (4)$$

式中: $\sigma_{ji,j} = \partial \sigma_{ji} / \partial x_j$; σ_{ij} 为应力; f_i 为体力; ϵ_{ij} 为应变张量; ϵ_{kk} 为第一应变不变量; u_i 和 u_j 为位移; λ 、 G 为拉梅常数, $G = \frac{E}{2(1+\nu)}$,其中 E 为材料的杨氏模量, ν 为材料的泊松比; α 为材料的线热膨胀系数; δ_{ij} 为单位张量。将上述平衡方程与几何方程代入本构方程,可得

$$-\dot{f}_i = \frac{E}{2(1+\nu)} \nabla^2 u_i + \frac{E}{2(1-2\nu)(1+\nu)} \frac{\partial \theta}{\partial x_i} - \frac{E\alpha}{1-2\nu} \frac{\partial(T - T_0)}{\partial x_i}, \quad (5)$$

式中: $\theta = \epsilon_x + \epsilon_y + \epsilon_z$,为体积应变。

除上述方程外,还需要考虑边界条件相似的关系。对于高速气流与激光联合作用下结构热-力响应特性的相似关系研究,可将高速气流的作用等效为气动力和气动换热边界条件^[20]。

考虑气动换热影响的激光辐照区域内的热边界条件为

$$\chi Q + h(T_w - T_\infty) - \sigma \epsilon T_w^4 = k \left(\frac{\partial T}{\partial n} \right), \quad (6)$$

式中: χ 为激光吸收系数; n 为换热表面的法线方向;

Q 为激光功率密度; h 为气体的对流换热系数; T_w 为壁温; T_∞ 为来流静温; σ 为玻尔兹曼常量; ϵ 为辐射系数; k 为材料的热导率。需要注意的是,本研究针对的是激光穿过近体流场后辐照金属材料诱导的热-力响应,仅需要考虑激光的近场传输特性。此时,激光传输路程较短,光束偏折、畸变、抖动等效应对激光在材料表面的分布产生的影响相对较小,因此可以忽略高速气流对激光传输的影响。此外,本研究中主要关注常用航空金属材料在发生熔融破坏前的热-力响应特性,最高壁温往往不超过 1000 K。在本研究中,与激光热流(约为 10⁶ W/m²)相比,辐射热流(约为 10⁴ W/m²)可以忽略不计。因此,激光辐照区域内的热边界条件可以简化为

$$\chi Q + h(T_w - T_\infty) = k \left(\frac{\partial T}{\partial n} \right). \quad (7)$$

在对流传热计算和实验中,通常用到的无量纲传热参数为斯托顿数 St 和努塞特数(Nu),其定义分别为

$$\begin{cases} St = \frac{Nu}{Re \cdot Pr}, \\ Nu = \frac{hl_0}{\lambda_{air}} \end{cases} \quad (8)$$

其中,

$$Re = \frac{\rho_\infty^{air} v_\infty l_0}{\mu}, \quad Pr = \frac{C_p^{air} \mu}{\lambda_{air}}, \quad (9)$$

式中: Re 为雷诺数; ρ_∞^{air} 为远场来流密度; v_∞ 为远场来流速度; l_0 为模型特征长度; μ 为气体黏性系数; Pr 为普朗特数; C_p^{air} 为气体的比定压热容; λ_{air} 为气体的热导率; h 为气体的对流换热系数。根据经验公式,Nusselt 数的近似公式可表达为

$$\begin{aligned} Nu &= St \cdot Re_x \cdot Pr = 0.332 Re_x^{\frac{1}{2}} Pr^{\frac{1}{3}} \left(\frac{\rho_{air}^{air*} \mu^*}{\rho_\infty^{air} \mu_\infty} \right)^{\frac{1}{2}} \\ &\quad (\text{laminar flow, } Re_x \leq 5 \times 10^5, 0.6 \leq Pr \leq 10) \\ Nu &= St \cdot Re_x \cdot Pr = 0.0296 Re_x^{\frac{4}{5}} Pr^{\frac{1}{3}} \left(\frac{\rho_{air}^{air*} \mu_\infty}{\rho_\infty^{air} \mu^*} \right)^{-\frac{1}{5}}, \\ &\quad (\text{turbulence, } 5 \times 10^5 < Re_x \leq 10^7, 0.6 \leq Pr \leq 60) \\ Nu &= St \cdot Re_x \cdot Pr = 0.185 Re_x^{\frac{1}{3}} \left(\lg \frac{\rho_{air}^{air*} \mu_\infty}{\rho_\infty^{air} \mu^*} Re_x \right)^{-2.584} \\ &\quad (\text{turbulence, } 10^7 < Re_x, 0.6 \leq Pr \leq 60) \end{aligned} \quad (10)$$

式中: ρ_{air}^{air*} 和 μ^* 分别为当地气体密度和黏性系数。

此时,结合方程(8)~(10),可以进一步推导得到努塞特数的表达式为

$$Nu = A Re_x^m Pr^n = A \left(\frac{\rho_\infty^{air} v_\infty l_0}{\mu} \right)^m \left(\frac{C_p^{air} \mu}{\lambda_{air}} \right)^n, \quad (11)$$

式中: A 、 m 、 n 等为常数, 由实验数据确定。

从而, 气体的对流换热系数可由无量纲传热参数表示为

$$h = \frac{Nu \cdot \lambda_{air}}{l_0} = \frac{A \left(\frac{\rho_0^{\text{air}} v_0 l_0}{\mu} \right)^m \left(\frac{C_p^{\text{air}} \mu}{\lambda_{air}} \right)^n \lambda_{air}}{l_0}, \quad (12)$$

式中的气体比定压热容 C_p^{air} 、气体黏性系数 μ 、气体热导率 λ_{air} 等气体参数随温度变化, 当温度场及来流速度不发生改变时, 气体的对流换热系数仅与 $\rho_0^{\text{air}} l_0$ 有关。

接下来考虑气动力影响的力边界条件。假设 P_i 为边界上在 i 方向上的表面力(压强), 则根据结构本构方程可得

$$\frac{2(1+\nu)}{E} P_i + \frac{2(1+\nu)}{1-2\nu} \alpha T = \nabla u_i + \frac{1}{1-2\nu} \theta_0. \quad (13)$$

可以发现, 当结构的材料不发生改变时, 力边界条件仅与 P_i 有关。

2.2 控制方程无量纲化

在建立控制方程组的基础上, 选取相关参数的无量纲量, 包括: $T' = \frac{T}{T_0}$, $t' = \frac{t}{t_0}$, $k' = \frac{k}{k_0}$, $\rho' = \frac{\rho}{\rho_0}$, $C' = \frac{C}{C_0}$, $f' = \frac{f}{f_0}$, $E' = \frac{E}{E_0}$, $\nu' = \frac{\nu}{\nu_0}$, $u' = \frac{u}{u_0}$, $\theta' = \frac{\theta}{\theta_0}$, $\alpha' = \frac{\alpha}{\alpha_0}$, $\chi' = \frac{\chi}{\chi_0}$, $Q' = \frac{Q}{Q_0}$, $P' = \frac{P}{P_0}$, $\mathbf{n}' = \frac{\mathbf{n}}{l_0}$ 。因此, 对控制方程(1)、(5)、(7)、(13)进行无量纲化, 得到

表 1 相似准则与准则说明
Table 1 Similarity criteria and guidelines

No.	Similarity criteria	Simplified conditions	Similarity criteria	Physical explanation
1	$\frac{k_0 t_0}{\rho_0 C_p l_0^2}$	The model materials are unchanged	$\frac{t_0}{l_0^2}$	The ratio of the laser irradiation time to the square of the geometric dimension is unchanged
2	$f_0 l_0$		$f_0 l_0$	The body force is multiplied by the geometric dimension
3	$\frac{E_0 u_0}{l_0}$	The model materials are unchanged	$\frac{u_0}{l_0}$	The deformation field is divided by the geometric dimension
4	$E_0 \theta_0$	The model materials are unchanged	θ_0	Strain fields are unchanged
5	$E_0 \alpha_0 T_0$	The model materials are unchanged	T_0	Temperature fields are unchanged
6	$\frac{\chi_0 Q_0 l_0}{k_0 T_0}$	The temperature fields and model materials are unchanged	$Q_0 l_0$	The laser power density is multiplied by geometric size
7	$\frac{A \left(\frac{\rho_0^{\text{air}} v_0 l_0}{\mu_0} \right)^m \left(\frac{C_p^{\text{air}} \mu_0}{\lambda_{air0}} \right)^n \lambda_{air0}}{k_0}$	The temperature fields, gas velocity and model materials are unchanged	$\rho_0^{\text{air}} l_0$	The density of gas is multiplied by geometric size
8	$\frac{P_0}{E_0 \theta_0}$	The strain fields and model materials are unchanged	ρ_0^{air}	The density of gas is unchanged

由表 1 可知, 在多场耦合条件下, 结构热载荷边界条件与力载荷边界条件的相似关系之间存在矛盾。因此, 理论上并不存在满足所有条件的相似律。然

$$\frac{\partial T'}{\partial t'} = \frac{k_0 t_0}{\rho_0 C_0 l_0^2} \frac{k'}{\rho' C'} \nabla^2 T', \quad (14)$$

$$-f_0 l_0 f' = \frac{E_0 u_0}{2(1+\nu_0 \nu') l_0} E' \nabla^2 u_i' + \frac{E_0 \theta_0}{2(1+\nu_0 \nu')(1-2\nu_0 \nu')} E' \frac{\partial \theta'}{\partial x_i'} - \frac{E_0 \alpha_0 T_0}{(1-2\nu_0 \nu')} E' \alpha' \frac{\partial T'}{\partial x_i'}, \quad (15)$$

$$A \left(\frac{\rho_0^{\text{air}} v_0 l_0}{\mu_0} \right)^m \left(\frac{C_p^{\text{air}} \mu_0}{\lambda_{air0}} \right)^n \lambda_{air0} h'(T_w' - T_\infty') = k' \left(\frac{\partial T'}{\partial n'} \right)_w, \quad (16)$$

$$\frac{2P_0(1+\nu_0 \nu')}{E_0 \theta_0} \frac{P'}{E'} + \frac{2(1+\nu_0 \nu')}{(1-2\nu_0 \nu')} \frac{\alpha_0 T_0}{\theta_0} \alpha' T' = \frac{u_0}{l_0 \theta_0} \nabla u_i' + \frac{1}{1-2\nu_0 \nu'} \theta', \quad (17)$$

式中: λ_{air0} 为气体的特征热导率, 一般为无穷远处来流气体的热导率。

2.3 相似准则归纳

为保证相似性, 需要统一方程中各个变量的系数。考虑到问题中不涉及模型材料的改变及材料的相变, 将无量纲方程组统一系数后可知, 两个相似的物理问题中应变场与温度场均无变化。因此, 对于各向同性材料, 其热物性参数及激光吸收系数随温度的变化不影响该问题的相似性^[22]。基于该结论将其他系数简化, 得到的相似准则与准则说明如表 1 所示。

而, 在高速气流与激光联合作用下, 温度梯度诱导的热应力往往远大于气动力作用产生的机械应力, 即切向气流带来的气动换热效应的影响远大于气动力效

应的影响^[20]。因此,本文重点考虑气动换热效应的相似性,忽略气动力的相似性。基于此,当模型尺寸变化至 α 倍时,可得到相关物理参数的尺度律,如表2所示。

表2 激光与气流联合作用下结构响应的尺度律(模型尺寸变化至 α 倍时)

Table 2 Scaling law of structural response under combined action of laser and airflow (when the dimension is scaled by α)

	Parameter	Scaling
Laser load	Laser beam diameter d_0	α
	Laser power density Q_0	$1/\alpha$
	Irradiation time t_0	α^2
Thermo-mechanical responses	Temperature T_0	1
	Deformation u_0	α
	Strain field θ_0	1
Parameters of high-speed airflow	Mach number Ma	1
	Static temperature T_s	1
	Static pressure P_s	$1/\alpha$
	Density ρ	$1/\alpha$
	Thermal conductivity λ_{air}	1
	Viscosity μ	1

表3 铝合金的热物性参数
Table 3 Thermophysical parameters of aluminum alloy

Temperature /K	Thermal conductivity / (W·m ⁻¹ ·K ⁻¹)	Specific heat / (J·kg ⁻¹ ·K ⁻¹)	Coefficient of thermal expansion /($10^{-6} \cdot K^{-1}$)	Young's modulus / GPa	Poisson's ratio	Density / (g·cm ⁻³)
293	155	900	21.4	68	0.31	2.85
373	159	921	23.1	64	0.31	2.85
473	163	1047	25.2	54	0.31	2.85
573	163	1130	26.8	42	0.31	2.85
673	159	1172	28.4	29	0.31	2.85

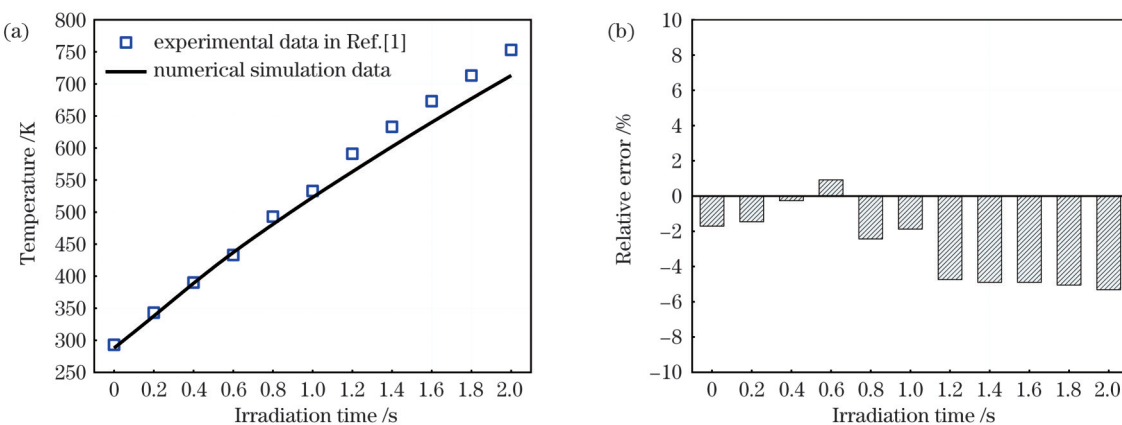


图1 多场耦合分析方法实验验证。(a)数值仿真与实验结果的温升历程对比;(b)误差

Fig. 1 Experimental validation of the multifield coupling analysis method. (a) Comparison for time evolution of temperature between simulated and experimental results; (b) error

而后,在如表 4 所列工况下开展数值仿真。本文主要考虑不同缩比率及不同马赫数两种情况下的对比验证。

(1) 针对 $Ma 3.0$ 气流, 对比工况 4(原模型)、5(1/2 模型)、6(1/2 模型, 未考虑气动相似)、7(1/4 模型)、8(1/4 模型, 未考虑气动相似), 验证不同缩比率下尺

度律的有效性;

(2) 对比工况 1($Ma 0.8$, 原模型)、2($Ma 0.8, 1/2$ 模型)、3($Ma 0.8, 1/2$ 模型, 未考虑气动相似)、4($Ma 3.0$, 原模型)、5($Ma 3.0, 1/2$ 模型)、6($Ma 3.0, 1/2$ 模型, 未考虑气动相似), 验证不同马赫数下尺度律的有效性。

表 4 仿真工况列表
Table 4 Simulation conditions

Condition No.	Mach number	Static pressure /Pa	Density / ($\text{kg} \cdot \text{m}^{-3}$)	Laser power density / ($\text{W} \cdot \text{cm}^{-2}$)	Irradiation time /s	Scaling
1	$Ma 0.8$	74130	1.01	188	10	1(real model)
2	$Ma 0.8$	148260	2.02	376	2.5	1/2
3	$Ma 0.8$	74130	1.01	376	2.5	1/2
4	$Ma 3.0$	74130	1.01	188	10	1(real model)
5	$Ma 3.0$	148260	2.02	376	2.5	1/2
6	$Ma 3.0$	74130	1.01	376	2.5	1/2
7	$Ma 3.0$	296520	4.04	752	0.625	1/4
8	$Ma 3.0$	74130	1.01	752	0.625	1/4

4 结果与讨论

4.1 不同缩比率下热-力响应尺度律验证

通过 $Ma 3.0$ 算例验证不同缩比率下结构热响应尺度律的有效性。图 2(a)给出了 1/2 缩比率下光斑中心的温升曲线, 图 2(b)给出了 1/4 缩比率下光斑中心的温升曲线。由于 $Ma 3.0$ 条件下的来流总温高于壁面温度, 气动加热效应占主导, 故未改变气流条件下的模型温度低于原模型。从图 2 中可以看出, 不同缩比

率下通过尺度律修正的温度演化历程均与原模型基本一致, 而未改变气流条件时即未考虑气动相似性时未能得到较好的拟合。而且, 随着尺度律增大, 换热效应差异增大, 未考虑气动相似性的曲线与原模型曲线的差异越发明显, 说明在实际缩比试验中有必要考虑多场耦合条件下的相似性。同时, 对于光斑中心温度, 满足相似关系的缩比模型与原模型的最大误差仅为 0.1%。这说明在进行不同缩比率条件下金属平板热响应考核与分析时, 所建立的尺度律是准确可靠的。

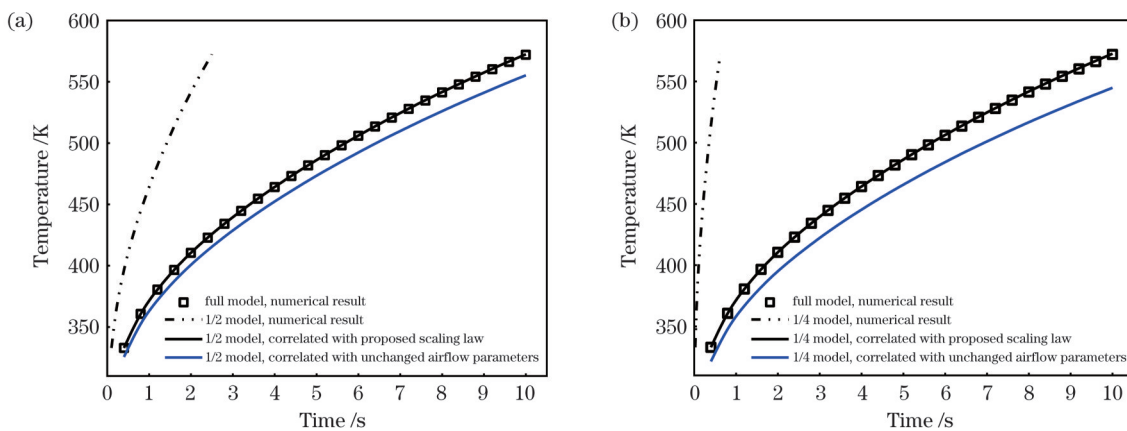


图 2 不同缩比率下光斑中心的温升曲线。(a) 1/2 缩比率;(b) 1/4 缩比率

Fig. 2 Temperature history curves of the laser spot center under different scaling factors. (a) 1/2 scaling; (b) 1/4 scaling

为验证不同缩比率条件下结构力响应尺度律的有效性, 得到了不同缩比率下温升结束时沿切向气流方向的应变分布, 如图 3 所示。可以看出, 经尺度律修正后的缩比模型的应变分布曲线与原模型曲线基本重合, 而未考虑气动相似性时未得到较好的拟合。而且, 随着尺度律增大, 未考虑气动相似性的应变曲线与原模型曲线的差异越发明显。对于等效弹性应变, 满足

相似关系的缩比模型与原模型的最大误差为 0.7%。这说明在进行切向气流与激光联合作用下金属平板力响应考核与分析时, 所建立的尺度律是准确可靠的。

此外, 图 4 给出了不同缩比率下模型的温度场及应变场对比云图。从温度场云图可以看出, 切向气流作用使得激光载荷辐照区域的温度沿着流线方向呈现不对称分布。总体来看, 原模型及缩比模型对应的温

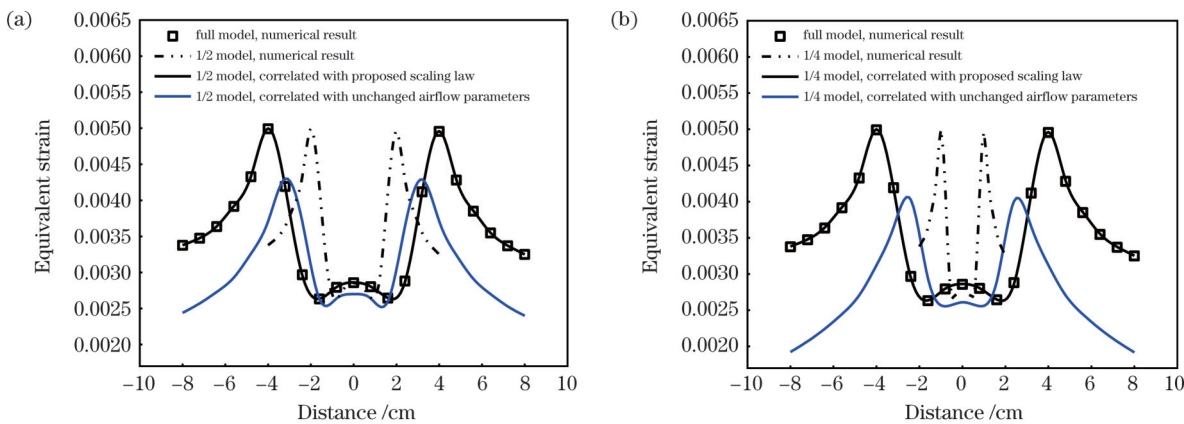


图 3 不同缩比率下沿气流方向的等效应变分布。(a) 1/2 缩比率;(b) 1/4 缩比率

Fig. 3 Equivalent strain passing through the direction of the airflow under different scaling factors. (a) 1/2 scaling; (b) 1/4 scaling

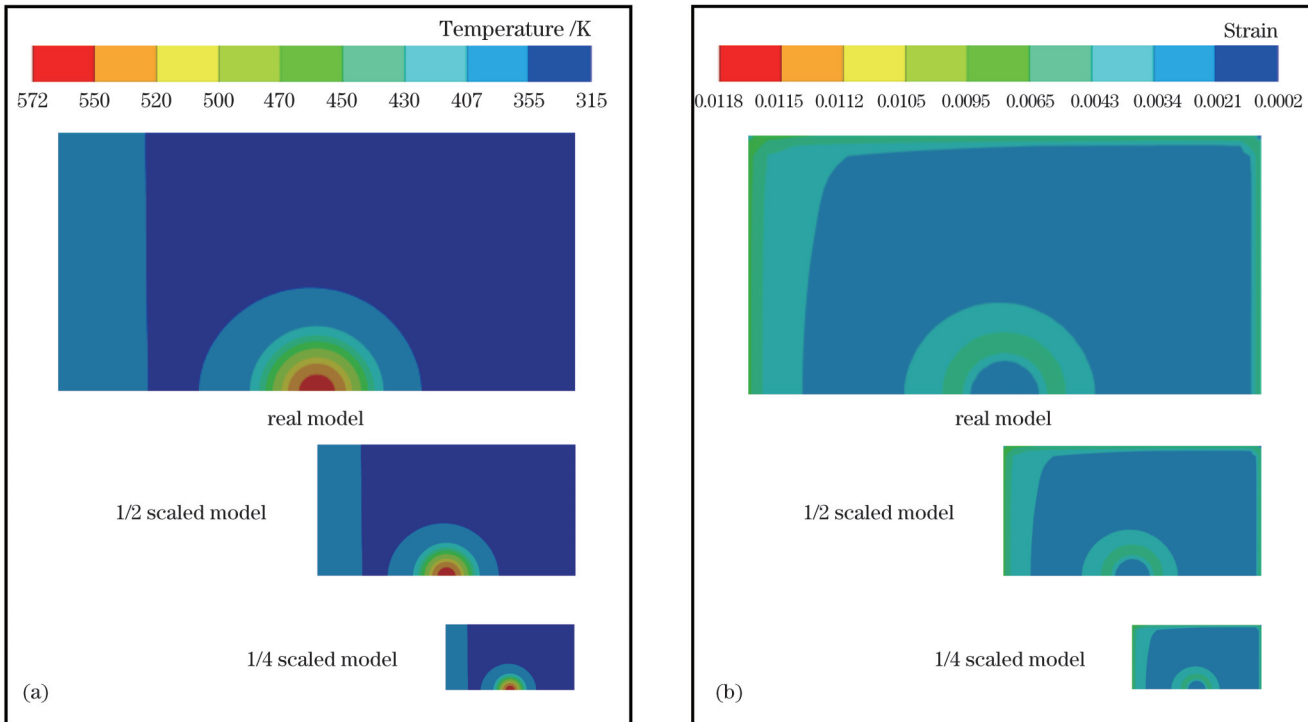


图 4 不同缩比率下金属平板温度及应变分布对比云图(半模型)。(a)温度场;(b)应变场

Fig. 4 Comparison of temperature and strain field diagrams of metal plate under different scaling factors (half model). (a) Temperature field; (b) strain field

度、等效弹性应变的大小与分布规律基本是一致的,均符合相应的尺度律,从而进一步验证了尺度律的准确性。

4.2 不同马赫数下热-力响应尺度律验证

为验证不同马赫数下结构热响应尺度律的有效性,计算得到了光斑中心的温升曲线,如图 5 所示。在 $Ma = 0.8$ 条件下,来流总温低于壁面温度,气动冷却效应占据主导;在 $Ma = 3.0$ 条件下,来流总温高于壁面温度,气动加热效应占主导。同时,可以看出,不同马赫数条件下通过尺度律修正的温升曲线与原模型曲线基本一致,而未考虑气动相似性时并未得到较好的拟合结果。而且,随着马赫数增大,换热效应增强,未考虑气动相似性的曲线与原模型曲线的差异越发明显。在

$Ma = 0.8$ 条件下,满足相似关系的缩比模型与原模型所得光斑中心温度的最大误差为 0.05%;在 $Ma = 3.0$ 条件下,满足相似关系的缩比模型与原模型所得光斑中心温度的最大误差为 0.07%。这说明在进行不同马赫数条件下金属平板热响应考核与分析时,所建立的尺度律是准确可靠的。

为验证不同马赫数下结构力响应尺度律的有效性,计算得到了温升结束时沿切向气流方向的轴向应变分布,如图 6 所示。可以看出,经尺度律修正后的轴向等效弹性应变分布曲线与原模型曲线基本重合,而随着马赫数增大,换热效应增强,未考虑气动相似性的曲线与原模型曲线的差异越发明显。在 $Ma = 0.8$ 条件下,满足相似关系的缩比模型与原模型所得切向气流

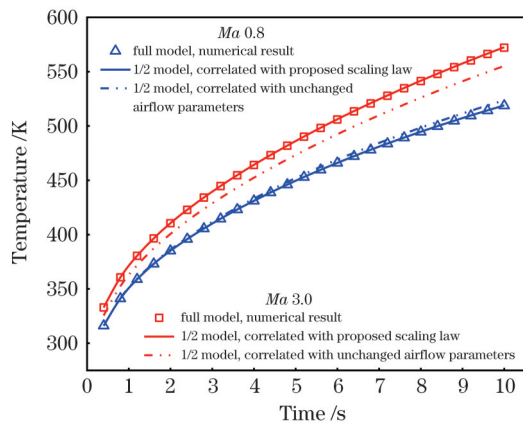


图 5 不同马赫数下光斑中心的温升曲线

Fig. 5 Temperature history curves of the laser spot center under different Mach numbers

方向的等效应变的最大误差为 0.36%；在 $Ma = 3.0$ 条件下，满足相似关系的缩比模型与原模型所得切向气流方向的等效应变的最大误差为 0.43%。这说明在进行切向气流与激光联合作用下金属平板力响应考核与分析时，所建立的尺度律是准确可靠的。

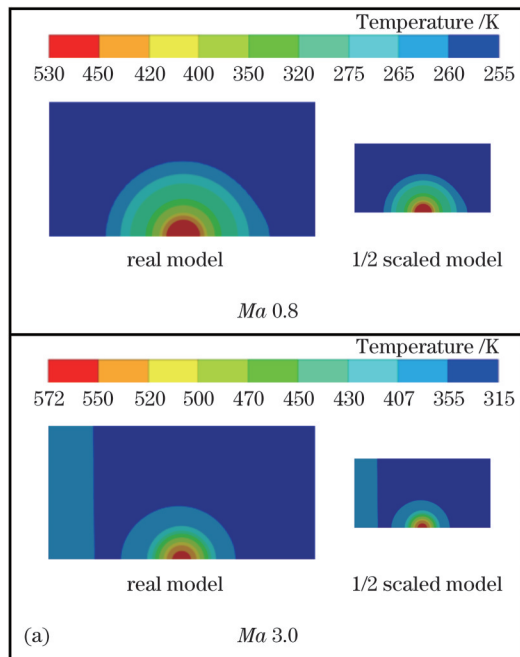


图 7 不同马赫数下金属平板温度及应变分布对比云图(半模型)。(a)温度场;

Fig. 7 Comparison of temperature and strain field diagrams of metal plate under different Mach numbers (half model). (a) Temperature field; (b) strain field

5 结 论

笔者开展了高速切向气流作用下激光辐照金属平板热-力响应相似关系的研究，明确了流-热-固多场耦合条件下金属平板热-力响应的尺度律，并通过数值算例对尺度律的有效性进行了考核验证，相关研究结果可为高速气流作用下激光辐照效应缩比试验与规律研究提供基础支撑。本文得到的主要结论包括：

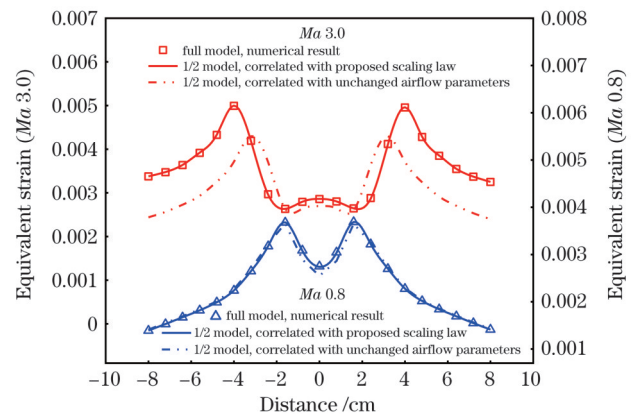


图 6 不同马赫数下沿切向气流方向的等效应变分布

Fig. 6 Equivalent strain passing through the direction of the airflow under different Mach numbers

图 7 给出了不同马赫数下金属平板温度及应变分布的对比云图。可以看出，原模型及缩比模型对应的温度、等效弹性应变的大小与分布规律基本一致，均符合相应的尺度律，从而进一步验证了尺度律的准确性。

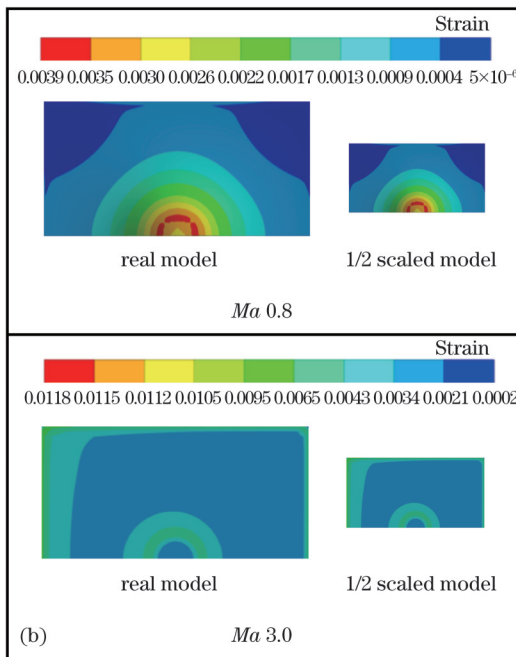


图 7 不同马赫数下金属平板温度及应变分布对比云图(半模型)。(b)应变场

1) 通过将高速气流的作用等效为力载荷和热载荷边界条件，建立了该耦合问题的基本控制方程，进而利用方程分析法推导出了适用于多场耦合条件下的热-力响应相似准则。

2) 根据该相似准则，气动引起的结构热载荷与力载荷边界条件的相似关系存在矛盾，无法同时满足。考虑到气流与强激光联合作用下的温度梯度诱导的热应力水平远大于气动力作用下产生的机械应力水平，

笔者重点考虑气动换热的相似性,忽略气动力的相似性,建立了相应的尺度律。

3) 通过高速气流下强激光辐照铝合金板的流-热-固多场耦合数值算例对所建立尺度律进行评估。结果表明,在不同的缩比率及马赫数条件下,缩比模型与原模型之间的热-力响应误差均小于 1%,验证了尺度律的可靠性。同时,随着缩比率增大或马赫数增大,气动换热效应增强,而未考虑气动相似性情况的缩比模型与原模型之间的热-力响应差异越发明显。

4) 本尺度律具有一定的适用范围:适用于热完全气体模型,对于高超声速流动以及空气在高温下发生离解、电离等多种复杂物理化学反应的情况,本尺度律不再适用;适用于平板流动问题,对于驻点、尖锥、复杂构型等无法应用平板公式的模型,本尺度律不再适用;适用于金属结构发生熔融前的热-力响应预测,金属结构发生熔融时本尺度律不再适用。

在工业与国防领域,高功率激光的辐照往往会导致金属材料发生熔融相变。高速气流下激光辐照金属材料诱导的熔融破坏问题涉及激光辐照、气动换热、氧化反应、金属熔凝、气动力“冲刷”等多种效应,是一个复杂的流-热-固-化多场耦合问题,目前研究人员对其中的相似关系尚不清楚。后续笔者拟将进一步利用量纲分析、数值模拟、试验验证等方法对该问题展开研究,确定该问题的主控因素,进而明确其热-力响应的相似关系。

参 考 文 献

- [1] Boley C D, Cutter K P, Fuchs S N, et al. Interaction of a high-power laser beam with metal sheets[J]. Journal of Applied Physics, 2010, 107(4): 043106.
- [2] Xing X D, Ma T, Wang R X, et al. Dynamic rupture of metal sheet subjected to laser irradiation and tangential subsonic airflow [J]. Theoretical and Applied Mechanics Letters, 2018, 8(4): 272-276.
- [3] 马特, 王江涛, 袁武, 等. 基于高温原位观测的高速风洞内强激光诱导的瞬态破坏行为研究[J]. 中国激光, 2023, 50(16): 1602201.
Ma T, Wang J T, Yuan W, et al. High temperature *in-situ* observation of high-power laser induced instantaneous damage behavior in high-speed wind tunnel[J]. Chinese Journal of Lasers, 2023, 50(16): 1602201.
- [4] 樊胜杰, 杨永强, 宋长辉, 等. 316L 不锈钢双激光选区熔化成形性能研究[J]. 中国激光, 2023, 50(16): 1602305.
Fan S J, Yang Y Q, Song C H, et al. Properties of 316L stainless steel formed by dual-laser selective melting[J]. Chinese Journal of Lasers, 2023, 50(16): 1602305.
- [5] 柴蓉霞, 田妍, 周新建, 等. 回字形扫描路径下高速激光熔覆数值模拟及实验研究[J]. 中国激光, 2023, 50(8): 0802205.
Chai R X, Tian Y, Zhou X J, et al. Numerical simulation and experimental study of high-speed laser cladding under circular scanning path[J]. Chinese Journal of Lasers, 2023, 50(8): 0802205.
- [6] 王一飞, 虞宙, 李康妹, 等. 纳秒激光烧蚀钛合金微坑形貌的数值模拟分析[J]. 中国激光, 2022, 49(8): 0802008.
Wang Y F, Yu Z, Li K M, et al. Numerical simulation of micro-pit morphology of titanium alloy ablated by nanosecond laser[J]. Chinese Journal of Lasers, 2022, 49(8): 0802008.
- [7] 杨剑波, 宗思光, 陈利斐. 高功率激光武器进展与启示[J]. 激光与红外, 2021, 51(6): 695-704.
Yang J B, Zong S G, Chen L F. Progress and enlightenment of high power laser weapons[J]. Laser & Infrared, 2021, 51(6): 695-704.
- [8] Young R L, Shanklin III R V. Thermal similarity study of a typical space vehicle element[J]. Journal of Spacecraft and Rockets, 1966, 3(12): 1796-1798.
- [9] 陈瑞. 大型航空航天结构缩比相似模型设计方法研究[D]. 大连: 大连理工大学, 2021.
Chen R. Research on design method of scale similarity model for large aerospace structures[D]. Dalian: Dalian University of Technology, 2021.
- [10] 岳军政, 吴先前, 黄晨光. 航行体出水破冰的多场耦合效应与相似律[J]. 力学学报, 2021, 53(7): 1930-1939.
Yue J Z, Wu X Q, Huang C G. Multi-field coupling effect and similarity law of floating ice break by vehicle launched underwater [J]. Chinese Journal of Theoretical and Applied Mechanics, 2021, 53(7): 1930-1939.
- [11] 陈发良, 余同希. 结构热力响应及失效的尺度律[J]. 固体力学学报, 1997, 18(1): 25-37.
Chen F L, Yu T X. Scaling laws for structural thermal-dynamic response and failure[J]. Acta Mechanica Solida Sinica, 1997, 18(1): 25-37.
- [12] 孙承纬. 激光辐照效应[M]. 北京: 国防工业出版社, 2002.
Sun C W. Laser irradiation effects[M]. Beijing: National Defense Industry Press, 2002.
- [13] 黄晨光, 陈思颖, 段祝平. 激光辐照下充压圆筒变形的相似律问题[J]. 强激光与粒子束, 2004, 16(8): 962-966.
Huang C G, Chen S Y, Duan Z P. Similarity criterion about deformation and failure of pressurized cylinder subjected to laser irradiation[J]. High Power Laser & Particle Beams, 2004, 16(8): 962-966.
- [14] Ma T, Xing X D, Song H W, et al. On similarity criteria of thin-walled cylinder subjected to complex thermomechanical loads[J]. Thin-Walled Structures, 2018, 132: 549-557.
- [15] 王玉恒, 刘峰. 强激光辐照充压圆柱壳体热力效应的相似性数值模拟(I)[J]. 激光杂志, 2008, 29(5): 62-63.
Wang Y H, Liu F. Numerical simulation on similarity of thermal-mechanical effects of cylindrical shells subjected to inner pressure and irradiated by intense laser(I)[J]. Laser Journal, 2008, 29(5): 62-63.
- [16] 李成龙, 汤伟, 邵俊峰, 等. 强激光辐照 7075 铝合金热响应与材料尺度律关系研究[J]. 激光与红外, 2020, 50(7): 789-794.
Li C L, Tang W, Shao J F, et al. Thermal response of 7075 aluminum alloy with different scaling laws under high power laser [J]. Laser & Infrared, 2020, 50(7): 789-794.
- [17] 刘坤, 张庆霞, 孙淑伟, 等. 无人机用航空铝合金材料激光毁伤特性缩比实验研究[J]. 装备环境工程, 2022, 19(12): 66-72.
Liu K, Zhang Q X, Sun S W, et al. Scale experimental study on laser damage characteristics of aviation aluminum alloy materials for UAV[J]. Equipment Environmental Engineering, 2022, 19(12): 66-72.
- [18] 黄亿辉, 宋宏伟, 黄晨光. 超声速气流下强激光辐照靶体失效数值模拟[J]. 强激光与粒子束, 2013, 25(9): 2229-2234.
Huang Y H, Song H W, Huang C G. Numerical simulation of failure of target irradiated by high-power laser subjected to supersonic airflow[J]. High Power Laser and Particle Beams, 2013, 25(9): 2229-2234.
- [19] 张文杰, 蒙文, 李云霞, 等. 切向气流对激光辐照效应影响的研究进展[J]. 激光与光电子学进展, 2016, 53(4): 041403.
Zhang W J, Meng W, Li Y X, et al. Research progress of tangential airflow impacting on laser irradiation[J]. Laser & Optoelectronics Progress, 2016, 53(4): 041403.
- [20] 刘磊, 桂业伟, 杜雁霞, 等. 飞行器热防护结构的相似准则问题研究[J]. 实验流体力学, 2015, 29(3): 25-29.
Liu L, Gui Y W, Du Y X, et al. Study on the similarity criteria of aircraft thermal protection structures[J]. Journal of Experiments in

- Fluid Mechanics, 2015, 29(3): 25-29.
- [21] Ai Q, Wang W Z, Gong Y, et al. Study on similarity criteria for aerodynamic/thermal coupling analysis of the aircraft[J]. International Communications in Heat and Mass Transfer, 2021, 129: 105705.
- [22] 丁升, 王建国, 王玉恒, 等. 激光辐照热力耦合问题的相似性[J]. 强激光与粒子束, 2005, 17(9): 1331-1334.
- [23] Ding S, Wang J G, Wang Y H, et al. Similarity of thermo-mechanical effect induced by high energy laser beam[J]. High Power Laser & Particle Beams, 2005, 17(9): 1331-1334.
- Wang R X, Wang Z W, Zheng H W, et al. Comparison of strategies for coupled flow-thermal analysis of thermal protection system at hypersonic flight condition[J]. International Journal of Aeronautical and Space Sciences, 2020, 21(2): 347-362.

Scaling Law for Thermo-Mechanical Responses of Metal Plate Subjected to Laser Irradiation Under High-Speed Airflow Condition

Cui Yue^{1,3}, Wang Ruixing^{1,3*}, Ma Te^{1,3}, Yuan Wu^{1,2,3}, Song Hongwei^{1,2,3}, Huang Chengguang³

¹Key Laboratory for Mechanics in Fluid Solid Coupling Systems, Institute of Mechanics, Chinese Academy of Sciences, Beijing 100190, China;

²Key Laboratory of High Temperature Gas Dynamics, Institute of Mechanics, Chinese Academy of Sciences, Beijing 100190, China;

³School of Engineering Science, University of Chinese Academy of Sciences, Beijing 100049, China

Abstract

Objective Laser technology is extensively used in various fields, including additive manufacturing, removal processing, and laser weaponry. This technology has the potential to revolutionize battlefield dynamics through defensive and offensive applications. Research on laser irradiation under high-speed airflow provides a theoretical basis for efficient damage strategies and the protection of aircraft, this is crucial for deploying military laser systems. However, conducting real-scale model tests for large-scale engineering structures is challenging due to equipment limitations and testing environments. Additionally, wind tunnel tests with real-scale models are prohibitively expensive and time-consuming, preventing extensive testing. Consequently, scaled-model tests are often relied upon for regularity studies. Therefore, establishing a similarity relationship in the thermomechanical responses between real and scaled models under laser irradiation and high-speed airflow is a practical approach. Significant efforts have been made to understand the similarity theory of laser-induced thermomechanical behavior under static air conditions. Nonetheless, due to the complex fluid-thermal-structural interactions in high-speed airflow, the similarity criteria for thermomechanical responses in an airflow environment significantly differ from those in static air. In this study, we propose new similarity criteria and scaling laws suitable for the thermomechanical responses of a metal plate subjected to high-speed airflow and laser irradiation.

Methods To clarify the similarity relation of thermomechanical responses for metal plates under coupling conditions, the effects of the tangential airflow were equivalently converted to the structural force and thermal load boundary conditions using the approximate equivalence method, and the dimensionless governing equations of the coupling problem were established. Thus, combined with the analysis of dominant factors, the similarity criteria and scaling laws suitable for the thermomechanical responses of the metal plate under the combined action of a high-speed airflow and laser were determined. According to the similarity criteria, there is a contradiction in the similarity relationship between the thermal boundary condition and force boundary condition under the fluid-thermal-structural coupling effects, which cannot be satisfied simultaneously. Considering that the thermal stress induced by the temperature gradient is much greater than the mechanical stress due to the aerodynamic force under the combined action of high-speed airflow and laser irradiation, this study focused on the similarity of aerodynamic heat transfer, ignored that of the aerodynamic force, and established the corresponding scaling law. Then, a fluid-thermal-structural coupling numerical example of a metal plate irradiated by a high-power laser under tangential flow was conducted to verify the scaling law under different scale ratios and Mach numbers.

Results and Discussions The similarity criteria and scaling laws for the fluid-thermal-structural coupling analysis of the metal plate subjected to laser irradiation and high-speed airflow are presented in Tables 1 and 2, respectively. A numerical example of the fluid-thermal-structural coupling of a metal plate irradiated by a high-power laser under a tangential flow is conducted to verify the scaling law. The results show that under different scale ratios and Mach numbers, the predicted response errors between the scaled and original models are within 1%, which proves the reliability and accuracy of the scaling law. Simultaneously, with the increase in scale ratios or Mach numbers, the aerodynamic heat transfer effect is enhanced, making the thermal-mechanical response difference between the scaled model and real model more obvious when the aerodynamic similarity criteria are not considered.

Conclusions In this study, similarity criteria and scaling laws suitable for the thermomechanical responses of a metal plate under the combined action of a high-speed airflow and laser are determined. Several numerical examples are conducted and compared to verify the proposed similarity criteria and scaling laws. The main conclusions are as follows: (1) Using the approximate equivalence method and analysis of dominant factors, the effects of the tangential airflow are equivalently converted to structural force and thermal

load boundary conditions, and the similarity criteria and scaling laws are determined. Considering that the thermal stress induced by the temperature gradient is significantly greater than the mechanical stress caused by the aerodynamic force, this study focusses on the similarity of the aerodynamic heat transfer and ignores the similarity of the aerodynamic force. (2) A fluid-thermal-structural coupling numerical example of a metal plate irradiated by a high-power laser under tangential flow was conducted to verify the scaling laws under different scale ratios and Mach numbers. The results show that the predicted response errors between the scaled and original models are within 1%, which proves the reliability and accuracy of the scaling laws. (3) However, the scope of application of the proposed similarity criteria should be emphasized in the following aspects: the similarity criteria are applicable for calorically perfect gases. For hypersonic flows, complex chemical reactions occur at high temperatures, and the similarity criteria are no longer applicable. The similarity criteria are applicable for the plate flow condition. However, for the non-plate flow, such as the flow around a blunt-nosed bodies, the similarity criteria are no longer applicable. The similarity criteria are applicable to the thermal-mechanical responses of the metal structure before melting. When melting is involved, similarity criteria are no longer applicable.

Key words laser technique; scaling law; equation analysis; metal plate; multifield coupling; thermo-mechanical responses